

Conclusions physiques du White Paper

- Densité d'énergie et particules chargées
 - Densité d'énergie $\rightarrow 15 \text{ GeV}/\text{fm}^3$
 - Particules chargées \rightarrow saturation des gluons dans l'état initial ?
- Thermalisation
 - Production d'étrangeté en accord avec l'hypothèse d'un équilibre chimique.
 - Le flot elliptique observé indique un haut degré de collectivité.
 - Pas d'image consistante de la dynamique de la collision.
- Binarité
 - Effet Cronin en dAu \rightarrow CGC ?
 - Binarité des photons directs et du charme en AuAu \rightarrow compatible avec CGC ?
- Suppression à grand p_T
 - Suppression des hadrons croissante avec la centralité \rightarrow milieu dense
 - Hypothèse d'un milieu dense confirmée par les corrélations angulaires
- Production des hadrons
 - Différence de comportement protons/pions
 - Étude du méson $\Phi \rightarrow$ différence de comportement pas liée à la différence de masse
 - Observation d'un flot partonique \rightarrow différence de comportement liée au nombre de quarks
 - Corrélations des jets incompatibles avec modèles de recombinaison

Les données du White Paper

- Les périodes de prise de données
 - Le rapport porte sur les données des runs 01 – 02 – 03.
 - Pour les résultats des runs 04/05 → QM05

Run	Year	Species	$s^{1/2}$ [GeV]	$\int Ldt$	N_{tot}	p-p Equivalent	Data Size
01	2000	Au+Au	130	$1 \mu b^{-1}$	10M	$0.04 pb^{-1}$	3 TB
02	2001/2002	Au+Au	200	$24 \mu b^{-1}$	170M	$1.0 pb^{-1}$	10 TB
		p+p	200	$0.15 pb^{-1}$	3.7G	$0.15 pb^{-1}$	20 TB
03	2002/2003	d+Au	200	$2.74 nb^{-1}$	5.5G	$1.1 pb^{-1}$	46 TB
		p+p	200	$0.35 pb^{-1}$	6.6G	$0.35 pb^{-1}$	35 TB
04	2003/2004	Au+Au	200	$241 \mu b^{-1}$	1.5G	$10.0 pb^{-1}$	270 TB
		Au+Au	62	$9 \mu b^{-1}$	58M	$0.36 pb^{-1}$	10 TB
05	2004/2005	Cu+Cu	200	$3.06 nb^{-1}$	1.1B		
		Cu+Cu	62	$190.2 \mu b^{-1}$	425M		
		p+p	200	$3.78 pb^{-1}$			

Les articles/auteurs du White Paper

~35 articles et preprints

- First measurement of the dependence of the charged particle pseudo-rapidity density (Adcox *et al.*, 2001a) and the transverse energy (Adcox *et al.*, 2001b) on the number of participants in Au+Au collisions at $\sqrt{s_{NN}} = 130$ GeV; systematic study of the centrality and $\sqrt{s_{NN}}$ dependence of $dE_T/d\eta$ and $dN_{ch}/d\eta$ (Adler *et al.*, 2004g).
- Discovery of suppressed production for π^0 's and charged particles at high p_T in Au+Au collisions at $\sqrt{s_{NN}} = 130$ GeV (Adcox *et al.*, 2002a) and a systematic study of the scaling properties of the suppression (Adcox *et al.*, 2003); extension of these results to much higher transverse momenta in Au+Au collisions at $\sqrt{s_{NN}} = 200$ GeV (Adler *et al.*, 2003e, 2004a).
- Co-discovery (together with BRAHMS (Arsene *et al.*, 2003), PHOBOS (Back *et al.*, 2003) and STAR (Adams *et al.*, 2003a)) of absence of high- p_T suppression in d+Au collisions at $\sqrt{s_{NN}} = 200$ GeV (Adler *et al.*, 2003g).
- Discovery of the anomalously large proton and anti-proton yields at intermediate transverse momentum in Au+Au collisions at $\sqrt{s_{NN}} = 130$ GeV through the systematic study of π^{\pm} , K^{\pm} , p and \bar{p} spectra (Adcox *et al.*, 2002a); study of the scaling properties of the proton and anti-proton yields in Au+Au collisions at $\sqrt{s_{NN}} = 200$ GeV (Adler *et al.*, 2003d);
- Measurement of Λ 's and $\bar{\Lambda}$'s in Au+Au collisions at $\sqrt{s_{NN}} = 130$ GeV (Adcox *et al.*, 2002d); measurement of ψ 's at $\sqrt{s_{NN}} = 200$ GeV (Adler *et al.*, 2004l); measurement of deuteron and anti-deuteron spectra at $\sqrt{s_{NN}} = 200$ GeV (Adler *et al.*, 2004e).
- Measurement of Hanbury-Brown-Twiss (HBT) correlations in $\pi^+\pi^+$ and $\pi^-\pi^-$ pairs in Au+Au collisions at $\sqrt{s_{NN}} = 130$ GeV (Adcox *et al.*, 2002h) and 200 GeV (Adler *et al.*, 2004f), establishing that the "HBT puzzle" of $R_{out} \approx R_{side}$ extends to high pair momentum.
- First measurement of single electron spectra in Au+Au collisions at $\sqrt{s_{NN}} = 130$ GeV, suggesting that charm production scales with the number of binary collisions (Adcox *et al.*, 2002e); measurement of centrality dependence of charm production in Au+Au collisions at $\sqrt{s_{NN}} = 200$ GeV (Adler *et al.*, 2004h).
- Sensitive measures of charge fluctuations (Adcox *et al.*, 2002f) and fluctuations in mean p_T and transverse energy per particle (Adcox *et al.*, 2002b; Adler *et al.*, 2004d) in Au+Au collisions at $\sqrt{s_{NN}} = 130$ GeV and 200 GeV.
- Measurements of elliptic flow for charged particles from Au+Au collisions at $\sqrt{s_{NN}} = 130$ GeV (Adcox *et al.*, 2002c) and 62 GeV to 200 GeV (Adler *et al.*, 2004m) and identified charged hadrons from Au+Au collisions at $\sqrt{s_{NN}} = 200$ GeV (Adler *et al.*, 2003c).
- Extensive study of hydrodynamic flow, particle yields, ratios and spectra from Au+Au collisions at $\sqrt{s_{NN}} = 130$ GeV (Adcox *et al.*, 2004b).
- First observation of J/ψ production in Au+Au collisions at $\sqrt{s_{NN}} = 200$ GeV (Adler *et al.*, 2004k).
- Measurement of the nuclear modification factor for hadrons at forward and backward rapidities in d+Au collisions at $\sqrt{s_{NN}} = 200$ GeV (Adler *et al.*, 2004c).
- First measurement of the jet structure of baryon excess in Au+Au collisions at $\sqrt{s_{NN}} = 200$ GeV (Adler *et al.*, 2004n).
- First measurement of elliptic flow of single electrons from charm decay in Au+Au collisions at $\sqrt{s_{NN}} = 200$ GeV (Adler *et al.*, 2005b).
- First measurement of direct photons in Au+Au collisions at $\sqrt{s_{NN}} = 200$ GeV (Adler *et al.*, 2005c).
- Measurement of crucial baseline data on π^0 spectra (Adler *et al.*, 2003f), direct photon production (Adler *et al.*, 2005a), and J/ψ production (Adler *et al.*, 2004i) in p + p collisions at $\sqrt{s} = 200$ GeV.
- First measurement of the double longitudinal spin asymmetry A_{LL} in π^0 production for polarized p+p collisions at $\sqrt{s} = 200$ GeV (Adler *et al.*, 2004j).

Writing Group
Yasuyuki Akiba (chair)
Brian Cole
Shinichi Esumi
Barbara Jacak
Jamie Nagle
Craig Ogilvie
Richard Seto
Paul Stankus
Mike Tannenbaum
Itzhak Tserruya

Stefan Bathe (scientific secretary)

- *Arlene Christian University, Abilene, TX 79699, USA
- *Florida State University, Tallahassee, FL 32306, USA
- *Georgia State University, Atlanta, GA 30303, USA
- *Hiroshima University, Higashi-Hiroshima 739-8526, Japan
- *Institute for High Energy Physics (IHEP), Beijing, People's Republic of China
- *University of Illinois at Urbana-Champaign, Urbana, IL 61801, USA
- *Yonsei University, Seoul, 150-747, Korea
- *Columbia University, New York, NY 10027 and New Laboratory, Irvington, NY 10522, USA
- *Dagupan, CEA Saclay, F-91191, Gif-sur-Yvette, France
- *Eotvos University, H-1060 Budapest, Egry街 1, Hungary
- *ELTE, Eotvos Lorand University, H-117 Budapest, Pázmány P. s. 1/A, Hungary
- *Florida State University, Tallahassee, FL 32306, USA
- *Georgia State University, Atlanta, GA 30303, USA
- *Hiroshima University, Higashi-Hiroshima 739-8526, Japan
- *Institute for High Energy Physics (IHEP), Beijing, People's Republic of China
- *University of Illinois at Urbana-Champaign, Urbana, IL 61801, USA
- *Yonsei University, Seoul, 150-747, Korea
- *Joint Institute for Nuclear Research, 141080 Dubna, Moscow Region, Russia
- *KARI, Chonnam National University, Gwangju, 500-702, South Korea
- *Korea High Energy Accelerator Research Organization, Yuseong, 305-380, South Korea
- *KEK, High Energy Accelerator Research Organization, Tsukuba-shi, Ibaraki-ken 305-0851, Japan
- *KFKI Research Institute for Particle and Nuclear Physics (RMKI), H-1525 Budapest 112, P.O. Box 49, Hungary
- *Korea University, Seoul, 136-701, Korea
- *Russian Research Center "Kurchatov Institute", Moscow, Russia
- *Ryukyu University, Naha 900, Japan
- *Laboratoire Leprince-Ringuet, Ecole Polytechnique, CNRS-IN2P3, Route de Saclay, F-91191, Palaiseau, France
- *Lawrence Livermore National Laboratory, Livermore, CA 94550, USA
- *Los Alamos National Laboratory, Los Alamos, NM 87545, USA
- *LPC, University of Houston, TX 77002, USA
- *Department of Physics, Lund University, Box 118, SE-221 00 Lund, Sweden
- *McGill University, Montreal, Quebec H3A 2T8, Canada
- *Institut für Kernphysik, University of Münster, D-48449 Münster, Germany
- *Miyagi University, Yonago, Aomori 991-8505, Japan
- *Nagasaki Institute of Applied Science, Nagasaki-shi, Nagasaki 851-8510, Japan
- *University of New Mexico, Albuquerque, NM 87131, USA
- *New Mexico State University, Las Cruces, NM 88003, USA
- *Oak Ridge National Laboratory, Oak Ridge, TN 37831, USA
- *IPN-Orsay, Université Paris Sud, CNRS-IN2P3, BP 1, F-91190, Orsay, France
- *Peking University, Beijing, People's Republic of China
- *PNPI, Petersburg Nuclear Physics Institute, Gatchina, Russia
- *RIKEN (The Institute of Physical and Chemical Research), Wako, Saitama 351-0801, JAPAN
- *RIKEN BNL Research Center, Brookhaven National Laboratory, Upton, NY 11973-5009, USA
- *Physics Department, Rikkyo University, 3-21-1 Niishi-Debura, Toshima, Tokyo 171-8501, Japan
- *St. Petersburg State Technical University, St. Petersburg, Russia
- *Universidade de São Paulo, Instituto de Física, Caixa Postal 66318, São Paulo, SP 05389-000, Brazil
- *System Electronics Laboratory, Seoul National University, Seoul, South Korea
- *Chemistry Department, Stony Brook University, Stony Brook, NY 11794-3400, USA
- *Department of Physics and Astronomy, Stony Brook University, SUNY, Stony Brook, NY 11794, USA
- *SUBATECH (Ecole des Mines de Nantes, CNRS-IN2P3, Université de Nantes) BP 30322 - 44307, Nantes, France
- *University of Tennessee, Knoxville, TN 37996, USA
- *Department of Physics, Tokyo Institute of Technology, Tokyo, 152-8551, Japan
- *University of Tokyo, Tokyo, Japan
- *Institute of Physics, University of Tsukuba, Tsukuba, Ibaraki 305, Japan
- *Yonsei University, Yonsei, Seoul 150-747, Korea
- *Waseda University, Advanced Research Institute for Science and Engineering, 17 Kikui-cho, Shinjuku-ku, Tokyo 169-0014, Japan
- *Weizmann Institute, Rehovot 76100, Israel
- *Yonsei University, P.O. Box 150-747, Korea

PHENIX :
 ~500 collaborateurs
 • 60 institutions
PHENIX France :
 ~ 25 collaborateurs
 • 5 labos français



Le plan du White Paper

Abstract

Extensive experimental data from high-energy nucleus-nucleus collisions were recorded using the PHENIX detector at the Relativistic Heavy Ion Collider (RHIC). The comprehensive set of measurements from the first three years of RHIC operation includes charged particle multiplicities, transverse energy, yield ratios and spectra of identified hadrons in a wide range of transverse momenta (p_T), elliptic flow, two-particle correlations, non-statistical fluctuations, and suppression of particle production at high p_T . The results are examined with an emphasis on implications for the formation of a new state of dense matter. We find that the state of matter created at RHIC cannot be described in terms of ordinary color neutral hadrons.

- I. Densité d'énergie et particules chargées
- II. Thermalisation
- III. Binarité
- IV. Suppressions à grand p_T
- V. Production des hadrons

I. Densité d'énergie et particules chargées de l'étude des conditions initiales

A prerequisite for creating a quark-gluon plasma is producing a system with sufficiently large energy density. From both elementary estimates [22] and from extensive numerical studies in lattice QCD [11,10], the required density is known to be on the order of 1 GeV/fm³. Establishing that this energy density is created in RHIC collisions is a basic ingredient in establishing the creation of a QGP at RHIC.

1. Densité d'énergie
2. Distribution des particules chargées

I. Densité d'énergie et particules chargées de l'étude des conditions initiales

1. Estimation de la densité d'énergie

- Formule de Bjorken

$$\varepsilon_{Bj} = \frac{1}{\pi R^2 \tau_0} \frac{dE_T}{dy}$$

- habituellement $\tau_0 = 1 \text{ fm}/c$:

- AGS (AuAu) $\rightarrow \varepsilon_{Bj} = 1.5 \text{ GeV}/\text{fm}^3$
- SPS (PbPb) $\rightarrow \varepsilon_{Bj} = 2.9 \text{ GeV}/\text{fm}^3$
- **RHIC (AuAu) $\rightarrow \varepsilon_{Bj} = 5.4 \text{ GeV}/\text{fm}^3$**

- Estimation de τ_0 au RHIC

$$\tau_0 = \hbar / m_T$$

$$\frac{dE_T}{dy} = \langle m_T \rangle \frac{dN}{dy}$$

$$\Rightarrow \langle m_T \rangle = \frac{dE_T / dy}{dN / dy} \approx \frac{dE_T / d\eta}{dN / d\eta} = \frac{dE_T / d\eta}{dN_{ch} / d\eta} \times \frac{dN_{ch} / d\eta}{dN / d\eta} \approx 0.85 \times \frac{2}{3} \approx 0.57 \text{ GeV}$$

$$\langle m_T \rangle \sim 0.57 \text{ GeV} \rightarrow \tau_0 \sim 0.35 \text{ fm}/c$$

$$\text{Collisions centrales} \rightarrow dE_T/d\eta \sim 600 \text{ GeV} \rightarrow \varepsilon_{Bj} \sim 15 \text{ GeV}/\text{fm}^3$$

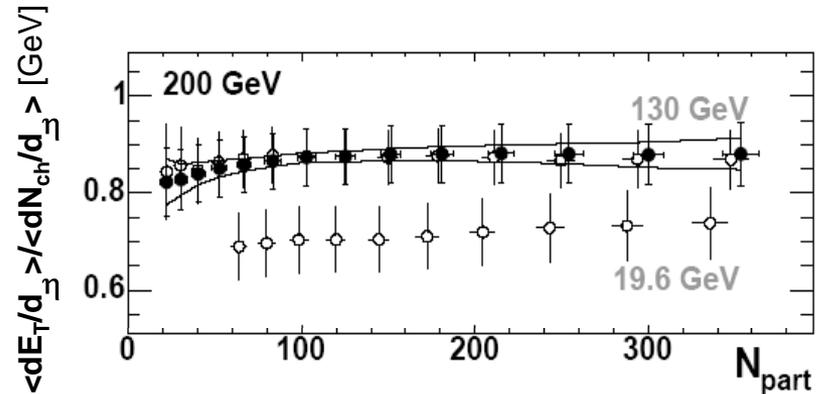
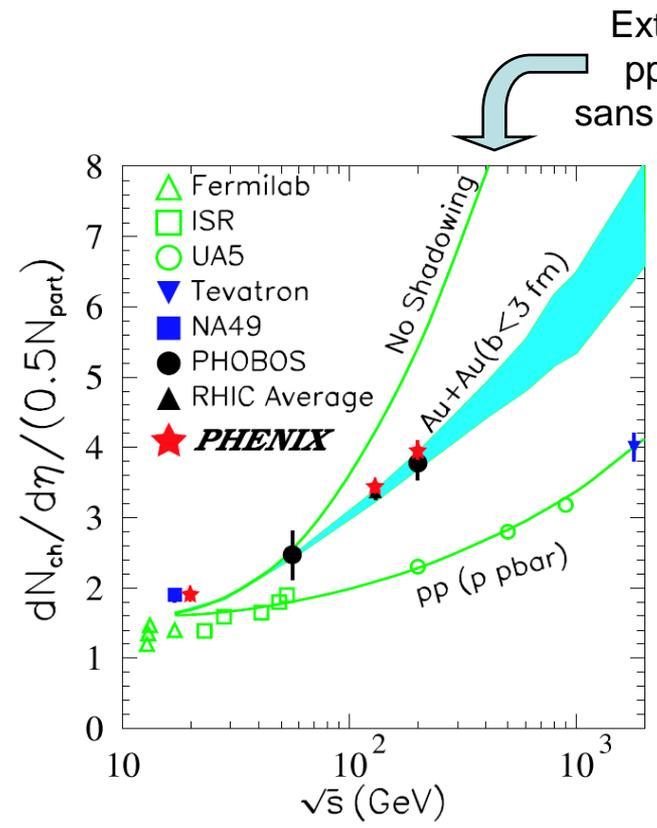


Fig. 6. The ratio of transverse energy density in pseudorapidity to charged particle density in pseudorapidity, at mid-rapidity; shown as a function of centrality, represented by the number of nucleons participating in the collision, N_{part} , for three different RHIC beam energies [67].

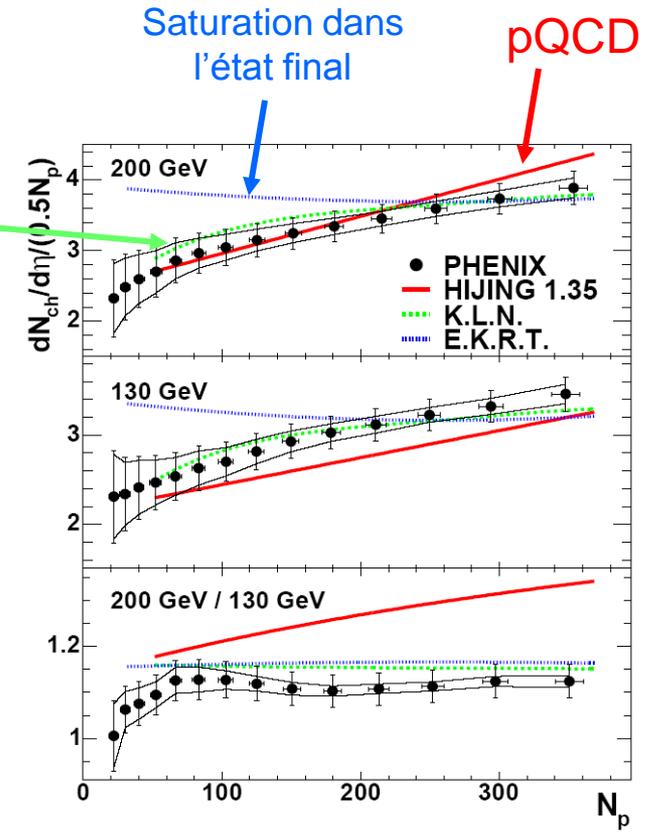
I. Densité d'énergie et particules chargées de l'étude des conditions initiales

2. Distribution des particules chargées



Li, Wang, Phys. Lett. B527 (2002) 85

Saturation des gluons dans l'état initial
Kharzeev-Levin-Nardi



Modification des pdf dans les noyaux
Saturation des gluons dans l'état initial → CGC ?

I. Densité d'énergie et particules chargées de l'étude des conditions initiales

- Conclusions

- The peak energy density in created secondary particles is at least $15 \text{ GeV}/\text{fm}^3$, and this is most likely an underestimate. This is well in excess of the $\sim 1 \text{ GeV}/\text{fm}^3$ required, according to lattice QCD predictions, to drive a QCD transition to QGP.
- Pre-RHIC expectations that E_T and charged particle production would be dominated by factorized pQCD processes were contradicted by data, which showed only very modest increases with centrality and beam energy. A new class of models featuring initial-state gluon saturation compares well with RHIC multiplicity and E_T data, and are also consistent with our Bjorken-style arguments for estimating energy densities at early times.

II. Thermalisation de l'étude du milieu produit

A key question is whether the matter formed at RHIC is thermalized, and if so when in the collision was equilibration achieved. If thermalization is established early then evidence for strong transverse expansion can be potentially related to the equation of state of the dense matter produced at RHIC.

1. Équilibre chimique
2. Expansion collective
3. Flot elliptique
4. Comparaison avec des modèles hydrodynamiques

II. Thermalisation de l'étude du milieu produit

1. Équilibre chimique

- La production des particules étranges permet de tester l'équilibre chimique.
- Les rapports K/π
 - Augmentent avec la centralité
 - Plus vite que p/π
 - **Évolution attendue par les modèles statistiques**

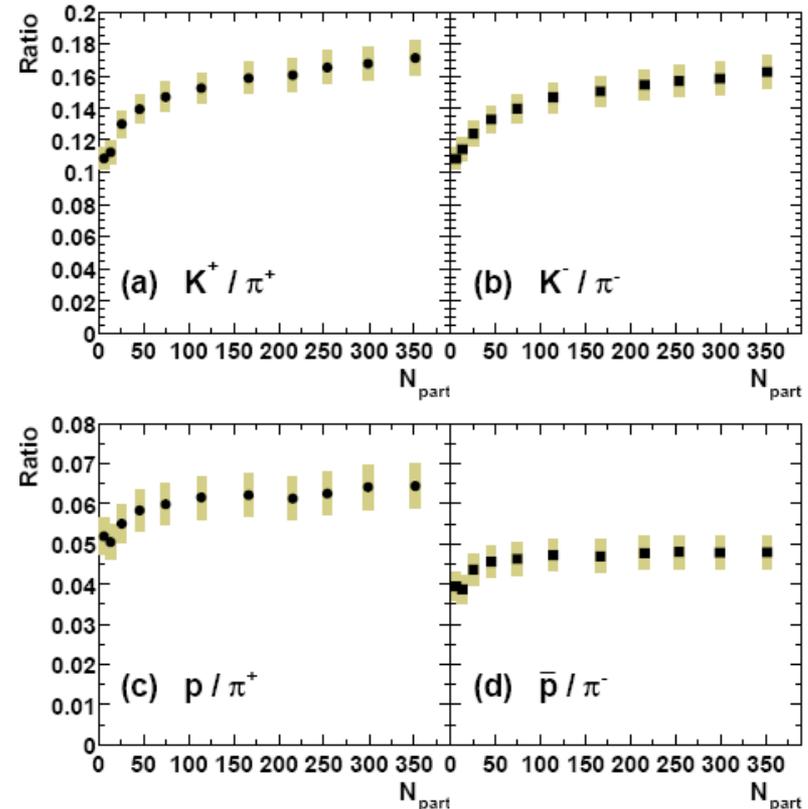


Fig. 9. Centrality dependence of particle ratios for (a) K^+/π^+ , (b) K^-/π^- , (c) p/π^+ , and (d) \bar{p}/π^- in Au+Au collisions at $\sqrt{s_{NN}} = 200$ GeV [54].

II. Thermalisation de l'étude du milieu produit

1. Équilibre chimique

- Dans les collisions AuAu (200 GeV) centrales
 - Les rapports d'abondance sont décrits par des modèles thermiques (Kaneta et Xu)
 - γ_S =étrangeté mesurée/étrangeté attendue (plein équilibre)
 - **On « mesure » :**
 - **T_{ch}=157 3 MeV**
 - **$\gamma_S=1.03 0.04$**
- Note : $\gamma_S \sim 1$ pour AGS et SPS

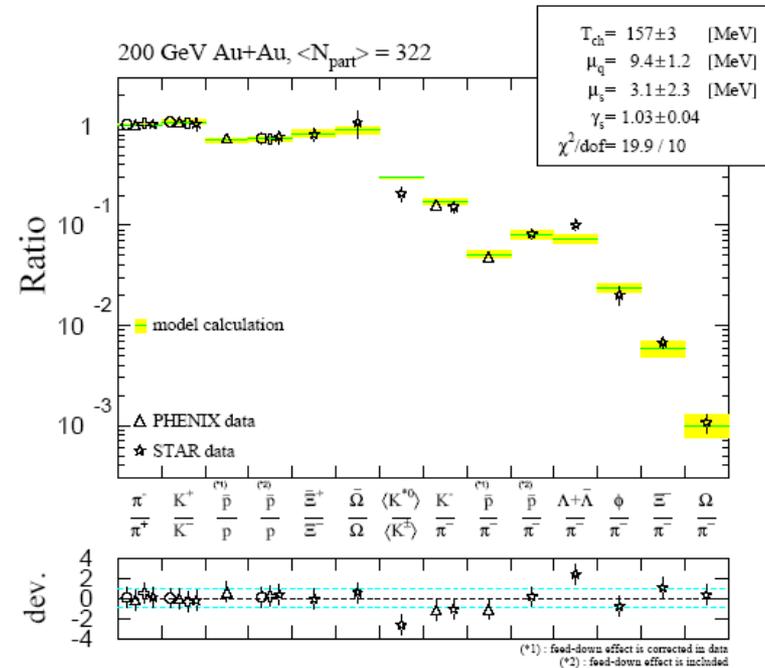


FIG. 10 Comparison of PHENIX (triangles), STAR (stars), BRAHMS (circles), and PHOBOS (crosses) particle ratios from central Au+Au collisions at $\sqrt{s_{NN}} = 200$ GeV at mid-rapidity. The thermal model descriptions from Kaneta and Xu (Kaneta and Xu, 2004) are also shown as lines. See Kaneta (Kaneta and Xu, 2004) for the experimental references.

II. Thermalisation de l'étude du milieu produit

2. Expansion collective

- $\langle p_T \rangle$ augmente plus fortement pour les protons
- Consistant avec une expansion collective $\rightarrow \langle p_T \rangle$ (m grand) > $\langle p_T \rangle$ (m petit)

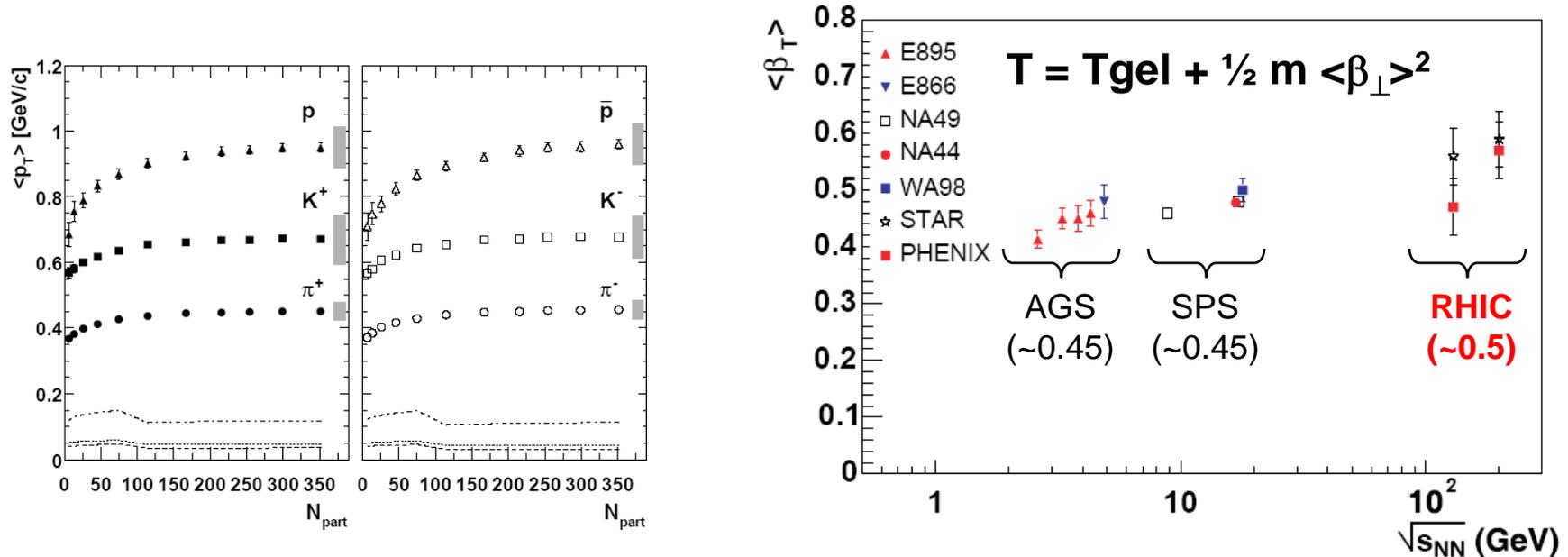
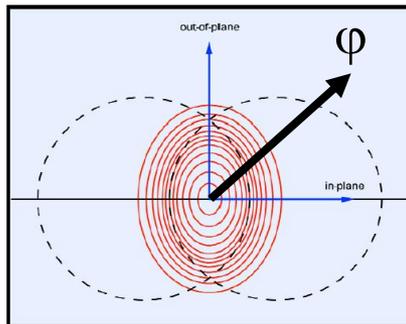
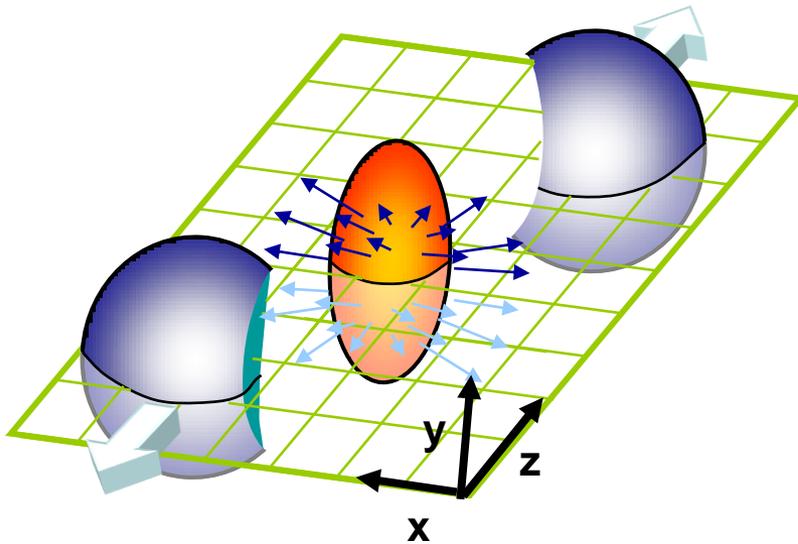


Fig. 13. Beam-energy dependence of the extracted mean transverse expansion velocity as a function of beam energy from simultaneous fits to spectra of different mass [97,98,99,100,101,48,102].

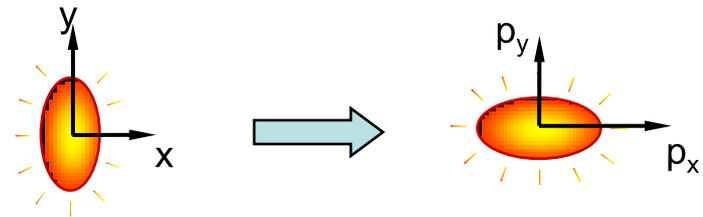
II. Thermalisation de l'étude du milieu produit

3. Flot elliptique



Dans un milieu fortement interagissant (thermalisé)

- Gradient de pression plus important dans le plan de la réaction
- Anisotropie spatiale \rightarrow anisotropie impulsionnelle



$$\frac{dN}{d\varphi dp_T} = 1 + v_2(p_T) \cos(2\varphi) \quad v_2 = \frac{\langle p_x^2 \rangle - \langle p_y^2 \rangle}{\langle p_x^2 \rangle + \langle p_y^2 \rangle}$$

$V_2 > 0 \rightarrow$ flot dans le plan de réaction

$V_2 < 0 \rightarrow$ flot hors du plan de réaction

II. Thermalisation de l'étude du milieu produit

3. Flot elliptique

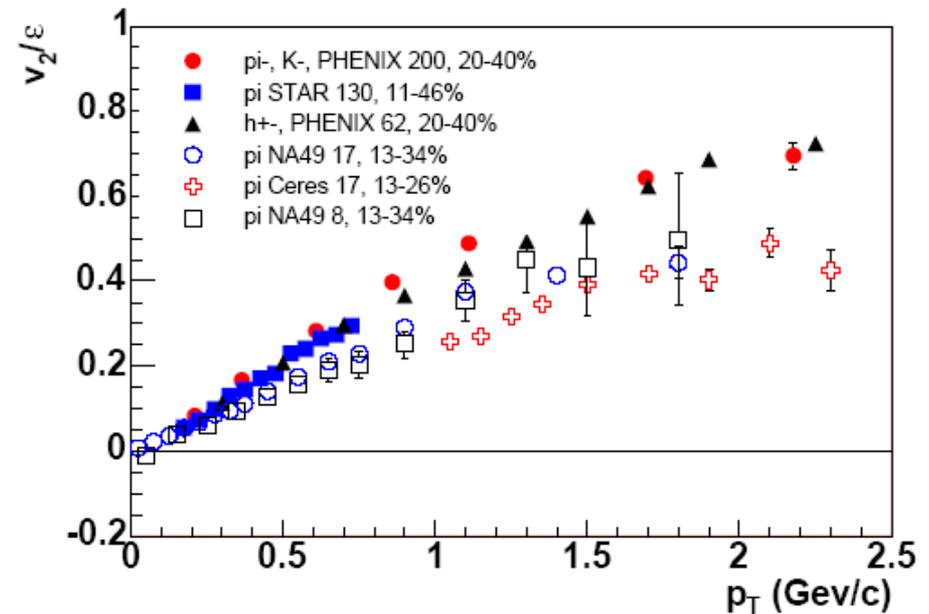
- $v_2 > 0 \rightarrow$ flot dans le plan de la réaction

- $v_2(\text{RHIC}) > v_2(\text{SPS})$

- v_2 reproduit par certains modèles hydrodynamiques

- $\tau_{\text{therm}} \sim 1 \text{ fm}/c$
- $\epsilon_{\text{init.}} > 10 \text{ GeV}/\text{fm}^3$
- $\epsilon_{\text{therm}} \sim 5 \text{ GeV}/\text{fm}^3$

$$\epsilon = \frac{\langle y^2 \rangle - \langle x^2 \rangle}{\langle y^2 \rangle + \langle x^2 \rangle}$$



L'excentricité spatiale dépend de la géométrie et du type de noyau

\rightarrow Modèle de Glauber

\rightarrow Pour comparer différentes espèces, normaliser v_2 par l'excentricité

II. Thermalisation de l'étude du milieu produit

4. Comparaison avec les modèles hydrodynamiques

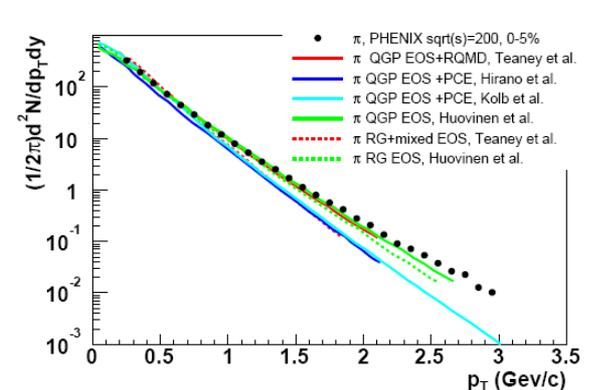
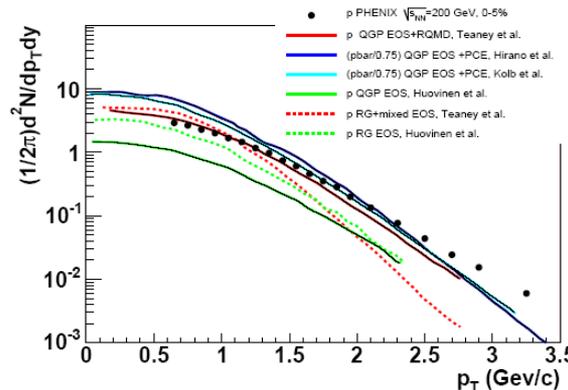
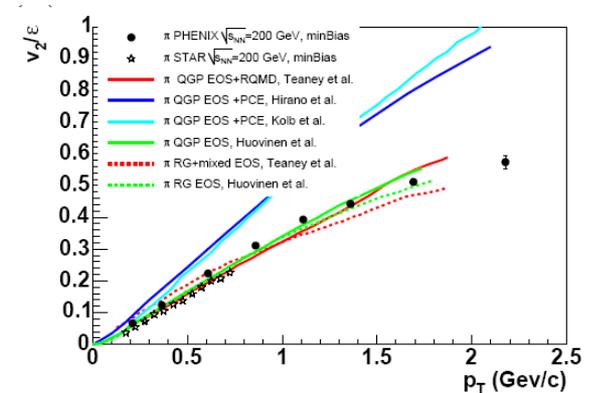
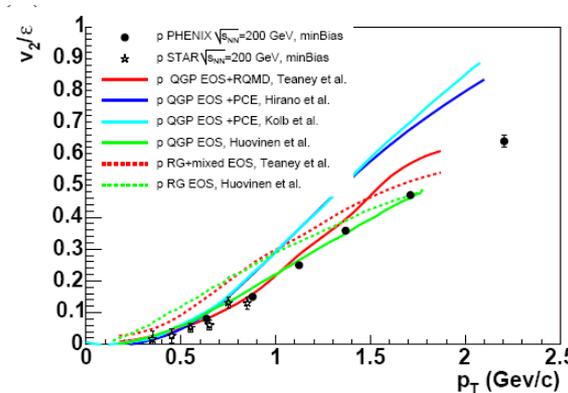
 Avec
 QGP


 Sans
 QGP

Un seul modèle
reproduit
« raisonnablement »
les données :

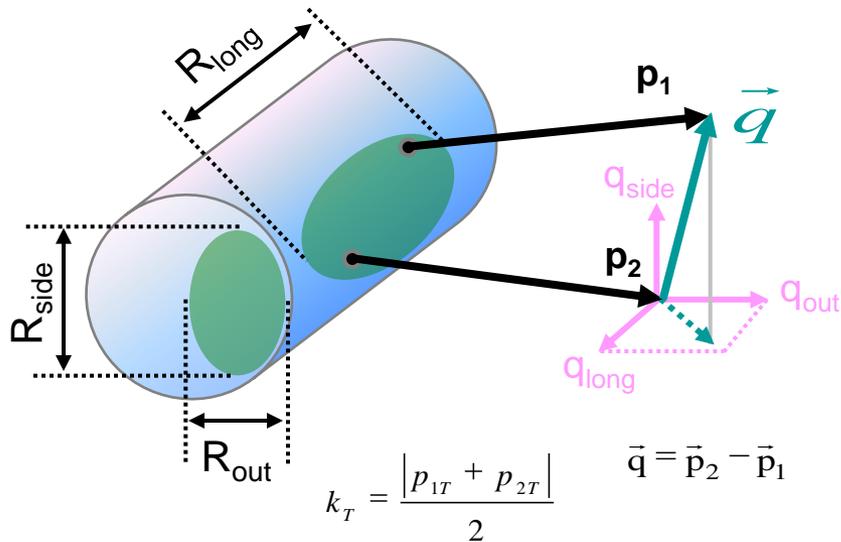
 QGP Teaney et al.

Modèle sans viscosité
(viscosité $\neq 0$ réduit v_2)

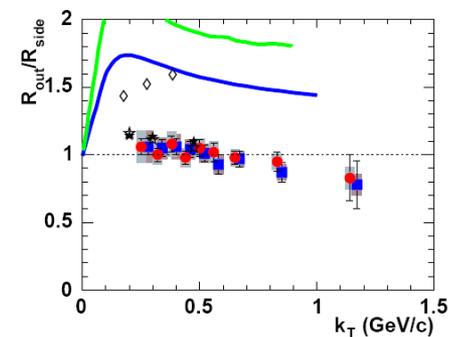
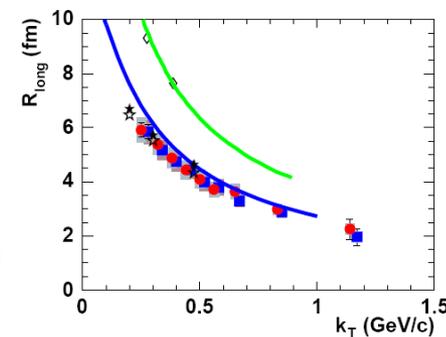
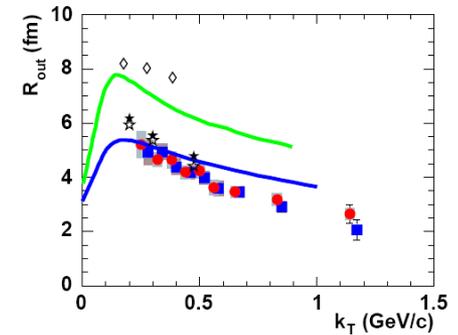
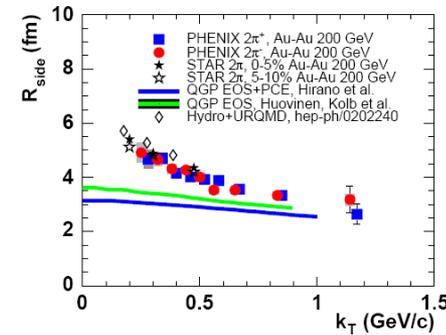


II. Thermalisation de l'étude du milieu produit

4. Comparaison avec les modèles hydrodynamiques : HBT



$$C_2 = 1 + \lambda \exp(-R_{\text{side}}^2 q_{\text{side}}^2 - R_{\text{out}}^2 q_{\text{out}}^2 - R_{\text{long}}^2 q_{\text{long}}^2)$$



- QGP Teaney ne fournit pas de prédiction pour HBT
- Deux autres modèles hydrodynamiques sont présentés → ne reproduisent pas les données

II. Thermalisation de l'étude du milieu produit

• Conclusions

- The measured yields and spectra of hadrons are consistent with thermal emission from a strongly expanding source.
- Strangeness is fully saturated at RHIC, consistent with full chemical equilibrium.
- The scaling of v_2 with eccentricity shows that collective behavior is established early in the collision.
- Elliptic flow is stronger at RHIC than at the SPS, since the measured slope of $v_2(p_T)$ for pions is 50% larger at RHIC.
- The measured proton $v_2(p_T)$ is less than that for pions at low p_T ; the small magnitude of the proton v_2 at low p_T is reproduced by hydro models that include both a QGP and hadronic phase.
- However several of the hydro models that reproduce the proton $v_2(p_T)$ fail for the pion $v_2(p_T)$.
- The HBT source parameters, especially the small value of R_{long} and the ratio $R_{\text{out}}/R_{\text{side}}$, suggest that the mixed phase is too long-lived in the current hydro calculations.

Hence we currently do not have a consistent picture of the space-time dynamics of reactions at RHIC as revealed by spectra, v_2 , and HBT. The lack of a

III. Binarité de l'étude des interactions dans l'état initial

- Processus proportionnels au nombre de collisions binaires ?

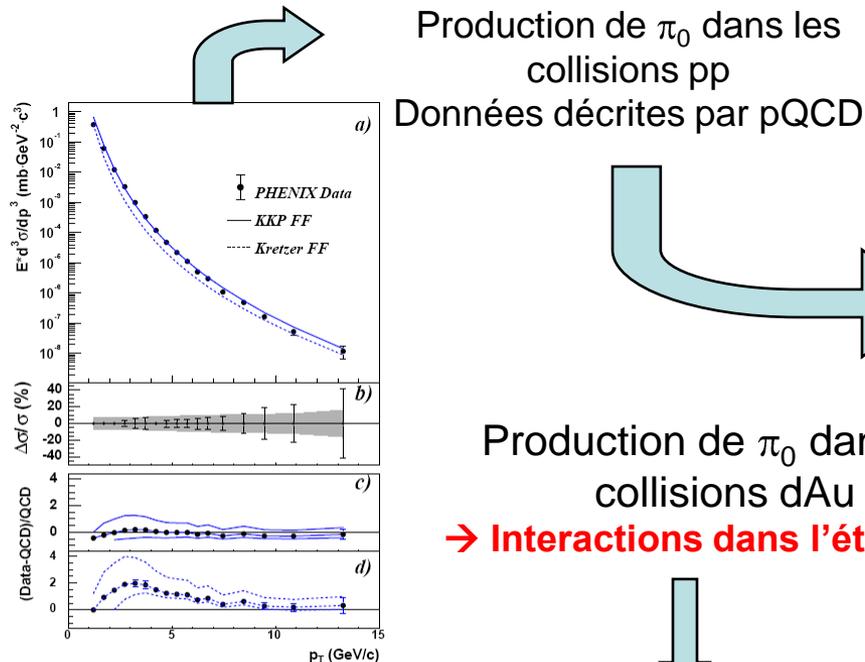


Fig. 27. PHENIX π^0 invariant cross section at mid-rapidity from $p+p$ collisions at $\sqrt{s} = 200$ GeV, together with NLO pQCD predictions from Vogelsang [151,152]. a) The invariant differential cross section for inclusive π^0 production (points) and the results from NLO pQCD calculations with equal renormalization and factorization scales of p_T using the “Klebl-Kramer-Pötter” (solid line) and “Kretzer” (dashed line) sets of fragmentation functions. b) The relative statistical (points) and point-to-point systematic (band) errors. c,d) The relative difference between the data and the theory using KKP (c) and Kretzer (d) fragmentation functions with scales of $p_T/2$ (lower curve), p_T , and $2p_T$ (upper curve). In all figures, the normalization error of 9.6% is not shown[60].

Production de π_0 dans les collisions dAu
→ Interactions dans l'état initial

Color Glass
Condensate ?

$$R_{CP} = \frac{dN^{centrale} / \langle N_{coll}^{centrale} \rangle}{dN^{périphérique} / \langle N_{coll}^{périphérique} \rangle}$$

RCP = 1 ↔ proportionnel

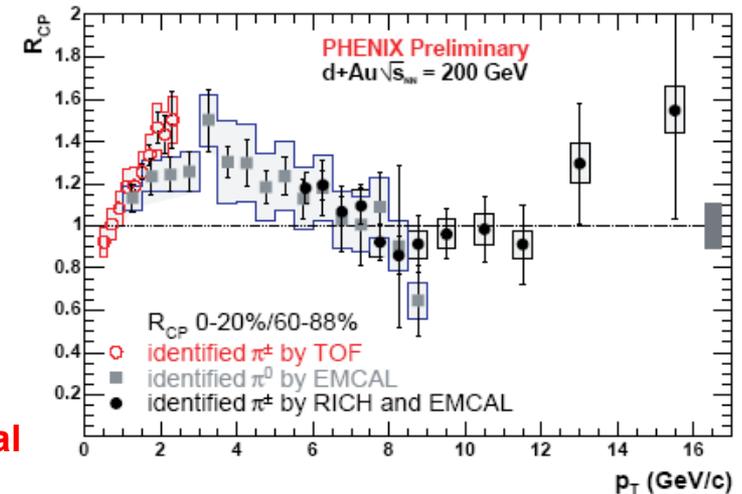
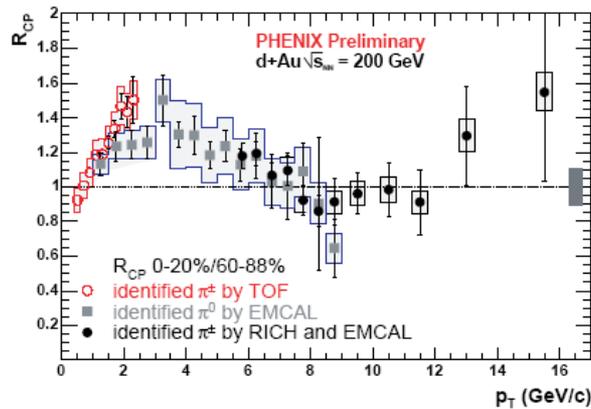


Fig. 32. Cronin effect in R_{CP} , the ratio of point-like scaled central to peripheral collisions for pions in $d+Au$ at $\sqrt{s_{NN}} = 200$ GeV[167]. Data points for low p_T are π^\pm identified by Time of Flight (TOF). Data at medium p_T are for π^0 identified by reconstruction in the Electromagnetic Calorimeter (EMCAL). Highest p_T data are for π^\pm identified by a count in the Ring Imaging Cherenkov Counter (RICH) and a deposited energy/momentum and shower shape in the EMCAL inconsistent with those of a photon or electron. The shaded band on the right represents the overall fractional systematic uncertainty due to N_{coll} .

III. Binarité de l'étude des interactions dans l'état initial

- Color glass condensate ?



Production de photons directs en AuAu proportionnelle au nombre de collisions

RCP anormal
En dAu

Production de charme en AuAu proportionnelle au nombre de collisions

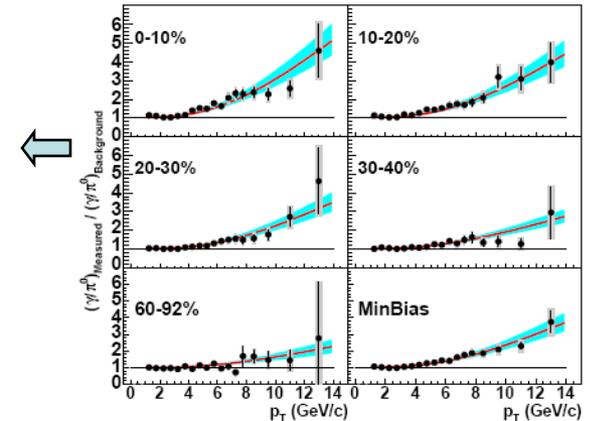


Fig. 33. PHENIX direct photon measurements relative to the background for for minimum bias and for five centralities of Au+Au collisions at $\sqrt{s_{NN}} = 200$ GeV (0-10% is the most central). Statistical and total errors are indicated separately on each data point by the vertical bar and shaded region, respectively. The curves represent a pQCD calculation of direct photons in $p + p$ collisions from Vogelsang [169,170,171,172] scaled to Au+Au assuming pure point-like (N_{coll}) scaling, with no suppression. The shaded region around the curves indicate the variation of the pQCD calculation for scale changes from $p_T/2$ to $2p_T$, plus the $\langle N_{coll} \rangle$ uncertainty [73].

The color glass condensate (CGC) provides an alternative view of the initial state of a nucleus at RHIC in which coherence of gluons due to non-linear gluon-gluon fusion can produce a Cronin-like effect, depending on the initial conditions and the kinematic range covered. However, at the present writing, there is no CGC description of the initial state nuclear structure function which reproduces the observed Cronin effect for pions in d+Au collisions and the observed binary scaling for both direct photon production and the total charm yield in Au+Au collisions.

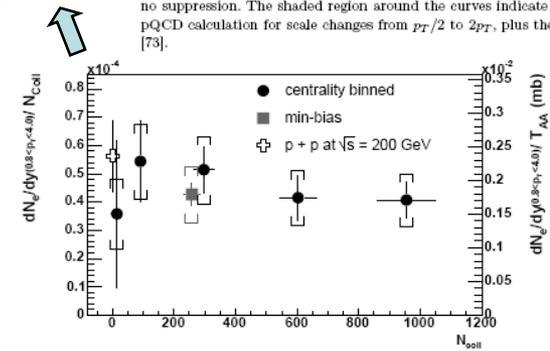


Fig. 34. Non-photon electron yield ($0.8 < p_T < 4.0$ GeV/c), dominated by semi-leptonic charm decays, measured in Au+Au collisions at $\sqrt{s_{NN}} = 200$ GeV scaled by N_{coll} as a function of N_{coll} . The right-hand scale shows the corresponding electron cross section per NN collision in the above p_T range. The yield in $p + p$ collision at 200 GeV is also shown [57].

IV. Suppression à grand p_T de l'étude de signatures (sondes) directes

To study the initial properties of the matter created in heavy ion collisions we need a probe that is already present at earliest times and that is directly sensitive to the properties of the medium. Partons resulting from hard scatterings during the initial crossing of the two nuclei in A+A collisions provide such a probe.

Energetic partons propagating through a dense medium are predicted to lose energy [173,174,175,176,177,178,179,180,181] thus producing a suppression in the yield of high- p_T hadrons produced from the fragmentation of these partons.

1. Suppression des hadrons
2. Corrélations angulaires

IV. Suppression à grand p_T de l'étude de signatures (sondes) directes

1. Suppression des π_0 dans les collisions centrales AuAu

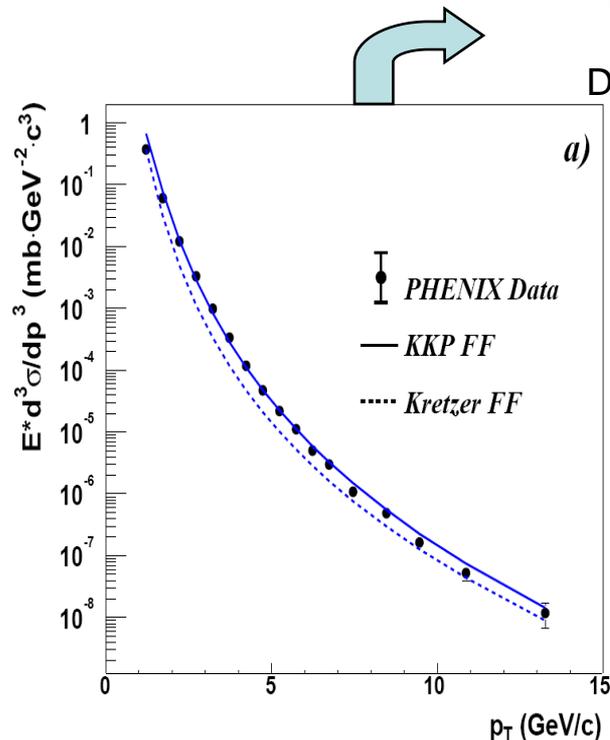


Fig. 27. PHENIX π^0 invariant cross section at mid-rapidity from $p+p$ collisions at $\sqrt{s} = 200$ GeV, together with NLO pQCD predictions from Vogelsang [151,152].

Production de π_0 dans les collisions pp
Données décrites par pQCD

Production de π_0 dans les collisions AuAu

→ Proportionnelle en AuAu périphériques

→ Forte suppression en AuAu centrales

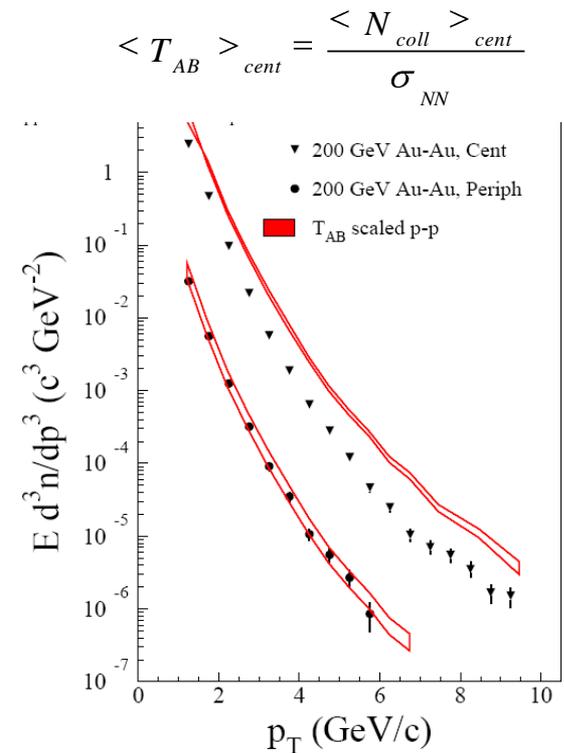


Fig. 35. π^0 p_T spectra in 200 GeV Au+Au collisions [49] compared to a T_{AB} scaling of the 200 GeV $p+p$ π^0 differential cross section [60]. The central data were obtained with a 0–10% centrality cut while the peripheral data were obtained with an 80–92% cut.

IV. Suppression à grand p_T de l'étude de signatures (sondes) directes

1. Suppression des π_0 dans les collisions centrales AuAu

- $$R_{AB} = \frac{dN_{AB}}{\langle N_{coll} \rangle \times dN_{NN}}$$
- dAu min bias
 - Léger défaut à bas $p_T \rightarrow$ les processus mous (bas p_T) ne sont pas proportionnels à T_{AB}
 - Léger excès à grand $p_T \rightarrow$ effet Cronin.
- AuAu périphériques
 - Léger défaut comparer à dAu (mais compatible)
- **AuAu centrales**
 - **Très forte suppression ($\sim x5$)**

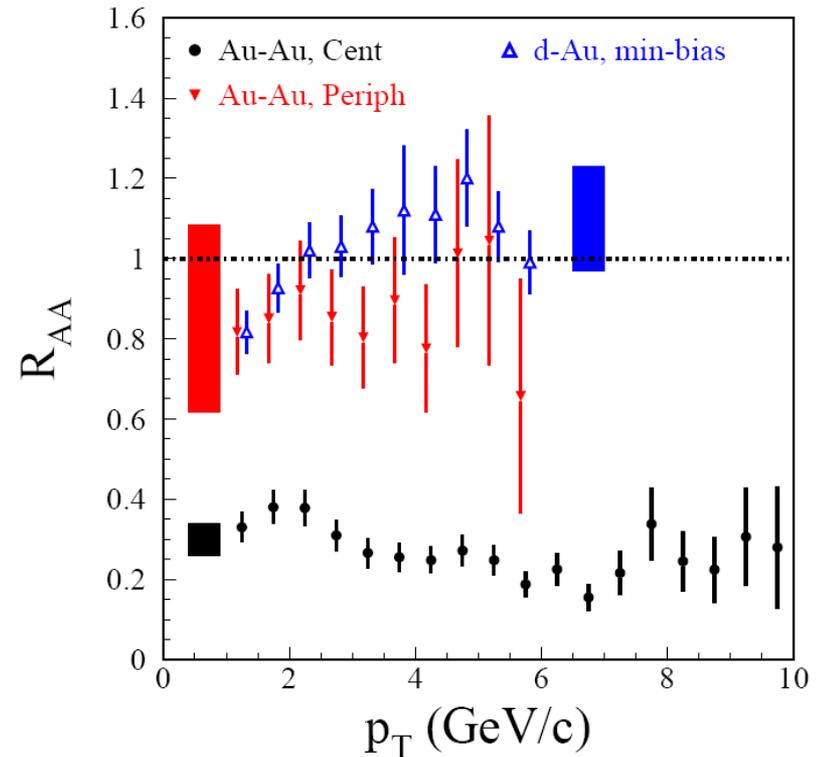
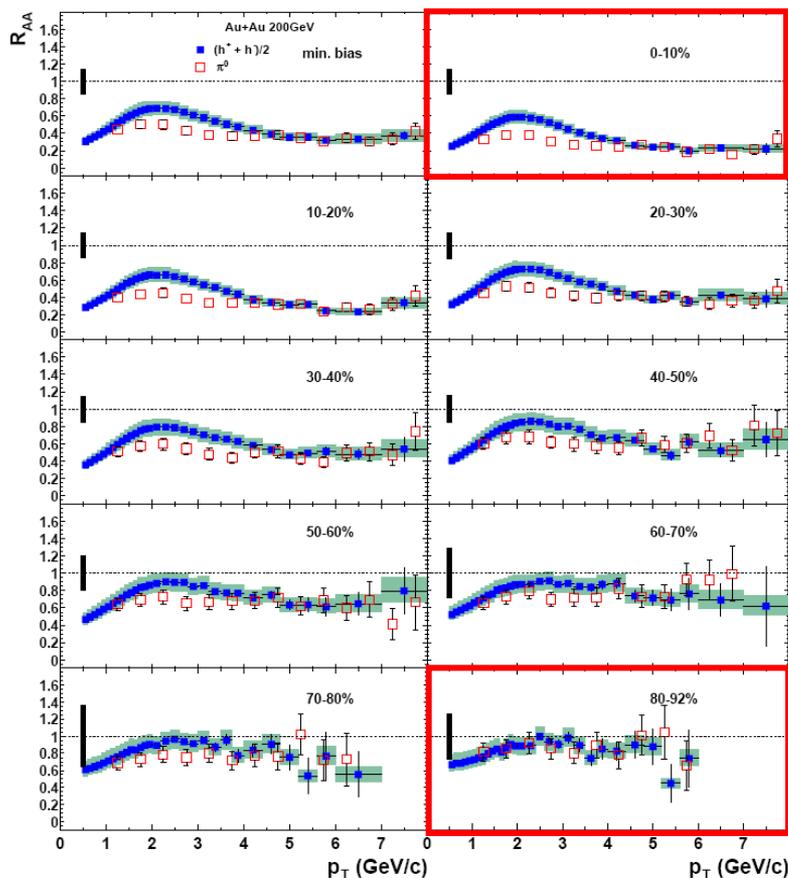


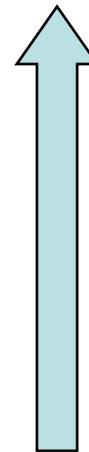
Fig. 36. π^0 $R_{AA}(p_T)$ for central (0–10 %) and peripheral (80–92 %) Au+Au collisions [49] and minimum-bias d+Au collisions [64]. The shaded boxes on the left show the systematic errors for the Au+Au R_{AA} values resulting from overall normalization of spectra and uncertainties in T_{AB} . The shaded box on the right shows the same systematic error for the d+Au points.

IV. Suppression à grand p_T de l'étude de signatures (évidences) directes

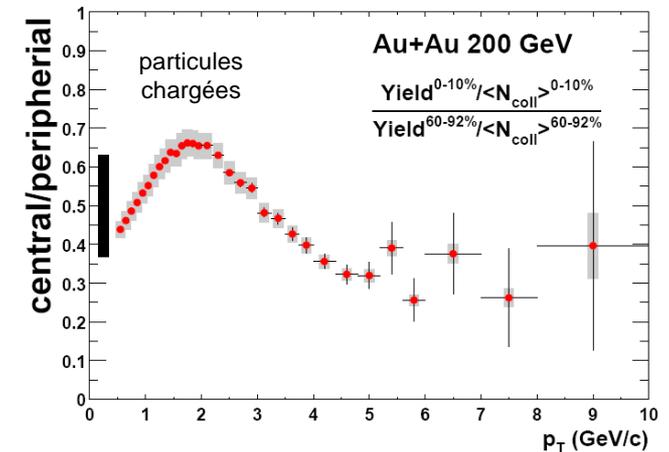
1. Suppression en fonction de la centralité



Les plus
centrales



Les plus
périphériques



**La suppression augmente
avec la centralité**

Note 1 : plus forte suppression des π_0 , comparés aux hadrons chargés, vers les p_T intermédiaires \rightarrow contribution des protons (cf. production des hadrons)

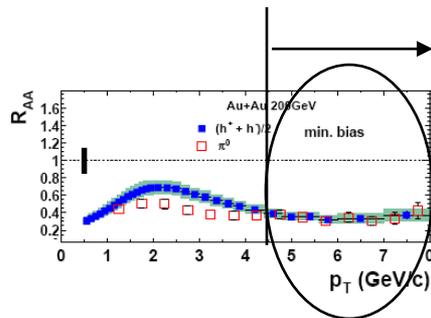
Note 2 : la suppression est constante pour $p_T > 4.5$ GeV/c



IV. Suppression à grand p_T de l'étude de signatures (évidences) directes

1. Suppression en fonction de la centralité

- Pour chaque tranche de centralité
 - Intègre le spectre pour $p_T > 4.5$ GeV/c
 - Représente la dépendance en fonction de N_{part}



The initial rise and subsequent decrease of $R_{AA}^{N_{part}}$ with increasing N_{part} suggests that the high- p_T hadron yield in Au+Au collisions has no simple dependence on N_{part} . The observation that the high- p_T yields initially increase proportional to T_{AB} demonstrates that in the most peripheral Au+Au collisions the hard-scattering yields are consistent with point-like scaling.

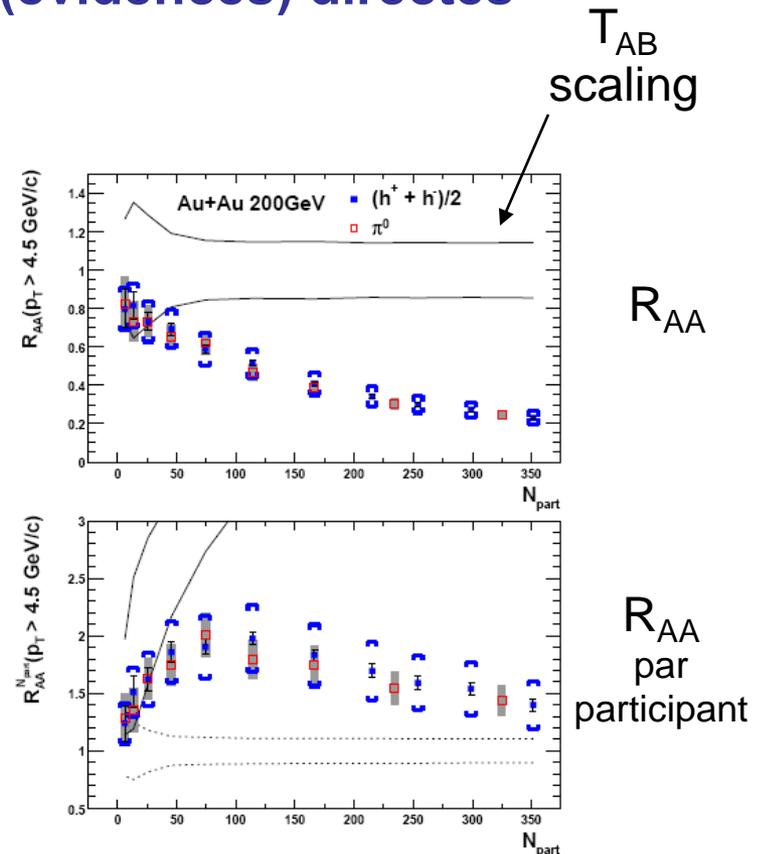


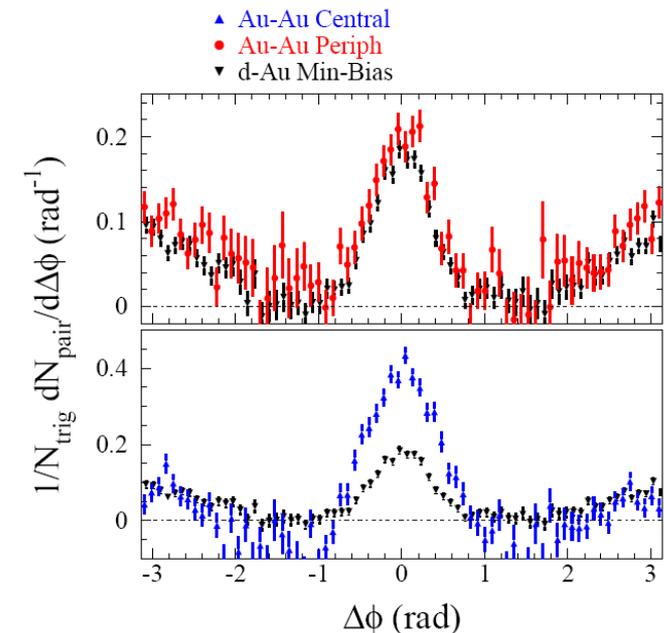
Fig. 38. Top panel: R_{AA} vs. N_{part} obtained from p_T -integrated ($p_T > 4.5$ GeV/c) Au+Au π^0 and charged-hadron spectra. The band indicates the systematic error bands on a hypothetical T_{AB} scaling of the $p + p$ p_T -integrated cross section. Bottom panel: π^0 and charged hadron yield per participant vs. N_{part} divided by the same quantity in $p + p$ collisions ($R_{AA}^{N_{part}}$). The solid band shows the same band as in the top panel expressed in terms of yield per participant pair while the dashed band indicates the systematic error bands around a hypothetical N_{part} scaling. Both plots are from [53].

IV. Suppression à grand p_T de l'étude de signatures (évidences) directes

2. Corrélations angulaires

a reasonable way to check the assumption that high- p_T hadron production in Au+Au collisions is due to hard scattering is to directly observe the angular correlations between hadrons in the jets.

- Particule « déclenchante » = $2.5 < p_T < 4$ GeV/c
- Particule « associée » = $1.0 < p_T < 2.5$ GeV/c
- $\Delta\Phi$ = angle azimuthal (déclenchante, associée)
- Interprétation :
 - $\Delta\Phi = 0 \rightarrow$ hadrons issus du même jet
 - $\Delta\Phi = \pi \rightarrow$ hadrons issus de jets différents
- Résultats :
 - dAu et AuAu périph sont en accord
 - AuAu centrales montrent un défaut de hadrons dans le jet opposé.



IV. Suppression à grand p_T de l'étude de signatures (évidences) directes

- Conclusions

The observed suppression of high- p_T particle production at RHIC is a unique phenomenon that has not been previously observed in any hadronic or heavy ion collisions at any energy. The suppression provides direct evidence that Au+Au collisions at RHIC have produced matter at extreme densities, greater than ten times the energy density of normal nuclear matter and the highest energy densities ever achieved in the laboratory. Medium-induced energy loss, predominantly via gluon bremsstrahlung emission, is the only currently known physical mechanism that can fully explain the magnitude and p_T dependence of the observed high- p_T suppression.

V. Production des hadrons de l'étude de l'hadronisation

One could conclude that a quark-gluon plasma had been formed if one had conclusive evidence of hadronization occurring from a thermal distribution of quarks and gluons.

1. Baryons et anti-baryons
2. Le méson Φ
3. Modèle hydrodynamique/recombinaison
4. Les corrélations des jets

V. Production des hadrons de l'étude de l'hadronisation

1. Baryons et anti-baryons

Rapports (anti)proton/pion
dans la région $2 < p_T < 5$
augmentation d'un facteur ~ 3
entre collisions centrales et
collisions périphériques.

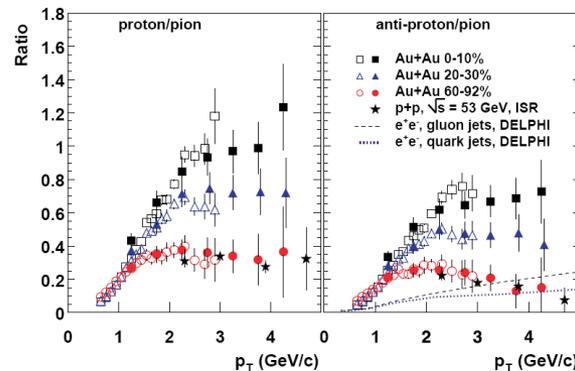


Fig. 44. p/π (left) and \bar{p}/π (right) ratios for central (0–10%), mid-central (20–30%) and peripheral (60–92%) Au+Au collisions at $\sqrt{s_{NN}} = 200$ GeV[52]. Open (filled) points are for $\pi^{+/-}$ (π^0), respectively. Data from $\sqrt{s} = 53$ GeV $p+p$ collisions [224] are shown with stars. The dashed and dotted lines are $(\bar{p} + p)/(\pi^+ + \pi^-)$ ratio in gluon and in quark jets [225].

Rapports hadron chargés/ π_0

- Forte augmentation pour $p_T \in [2:5]$
- Retour vers $p+p$ pour $p_T > 5$
- l'effet augmente avec la centralité
- Effet dû à la masse des hadrons ?
- Effet baryon-méson ?



mesuré
en $p+p$

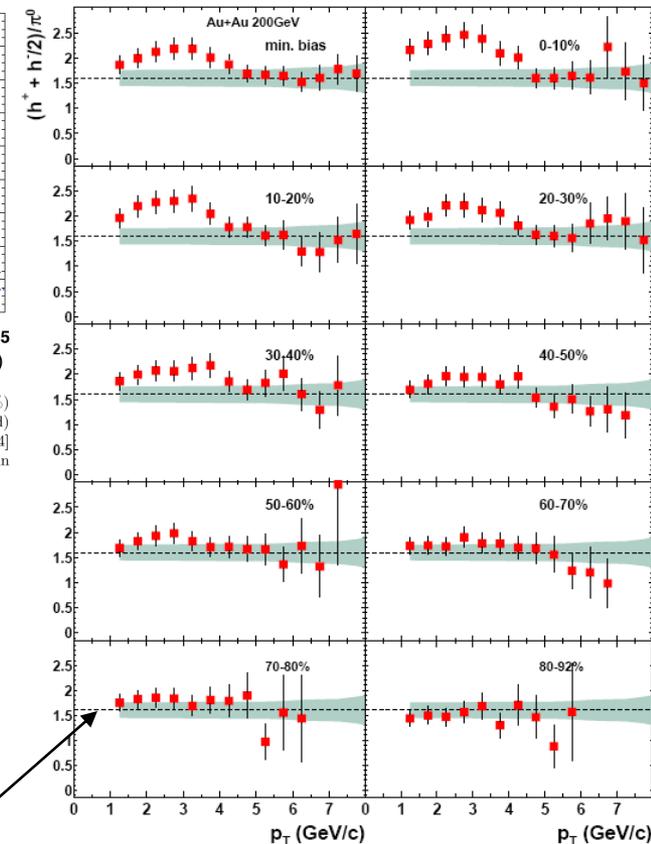


Fig. 45. Charged hadron to π^0 ratio for different centrality classes for Au+Au collisions at $\sqrt{s_{NN}} = 200$ GeV[53]. Error bars represent the quadratic sum of statistical and point to point systematic errors. The shaded band shows the normalization error common to all centrality classes. The line at 1.6 is the h/π ratio measured in $p+p$ collisions at $\sqrt{s} = 53$ GeV [224] and $e+e-$ collisions [225].

V. Production des hadrons de l'étude de l'hadronisation

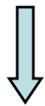
2. Le méson Φ

Le Φ :

- C'est un méson $\rightarrow \pi_0$
- $M \sim 1 \text{ GeV} \rightarrow$ proton

On observe :

- $R_{CP}(\Phi) = R_{CP}(\pi_0)$
- $R_{CP}(\Phi) \neq R_{CP}(\text{proton+antiproton})$



L'effet n'est pas dû à la masse



Effet baryon-méson ?

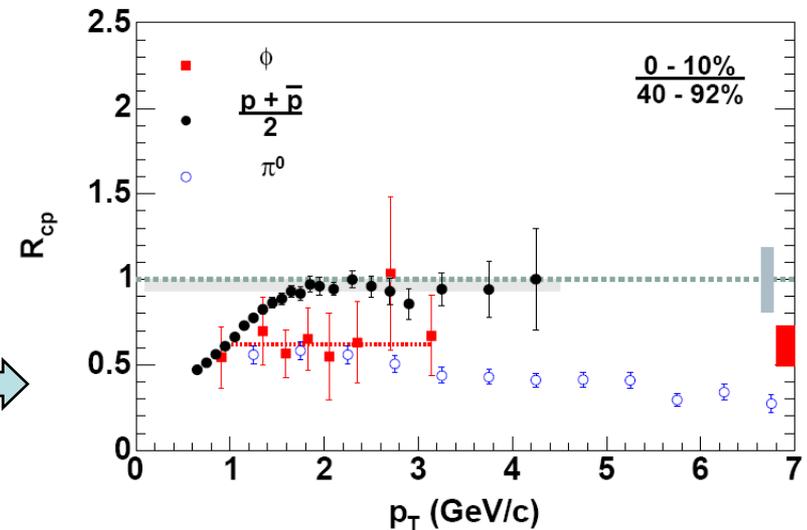


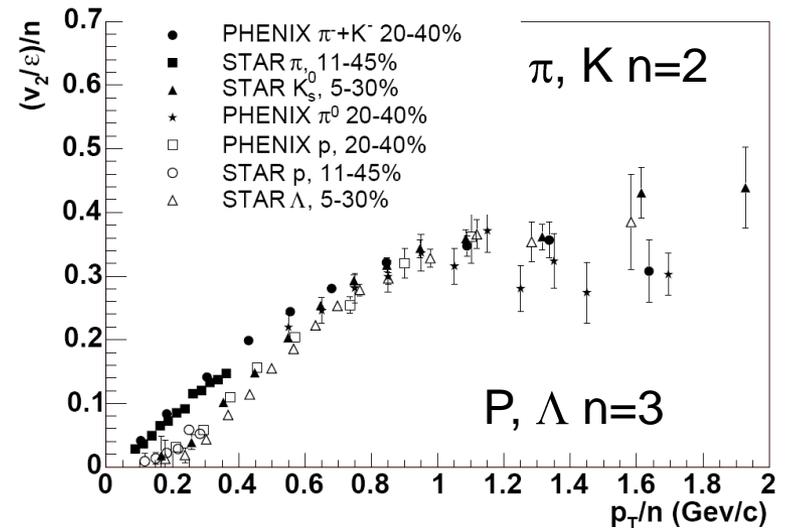
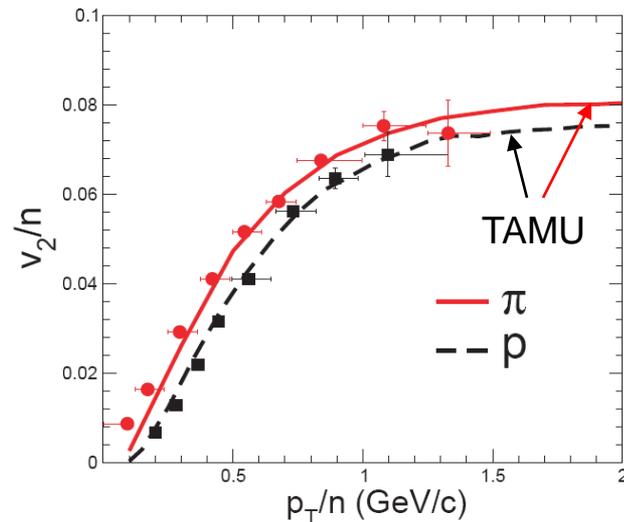
Fig. 48. The R_{CP} of the ϕ as measured in the KK channel, compared to the protons and pions for Au+Au collisions at $\sqrt{s_{NN}} = 200 \text{ GeV}$ [69].

V. Production des hadrons de l'étude de l'hadronisation

3. Modèle hydrodynamique/recombinaison

Effet baryon ($n_{\text{quarks}}=3$)/mésion ($n_{\text{quarks}}=2$) ?

Flot partonique observé
dans les données



Flot partonique reproduit
par un modèle de
recombinaison

Compatibilité hydrodynamique/recombinaison ?

V. Production des hadrons de l'étude de l'hadronisation

3. Modèle hydrodynamique/recombinaison

Hydrodynamique :

QGP Teaney décrit le rapport p/π jusqu'à 2 GeV

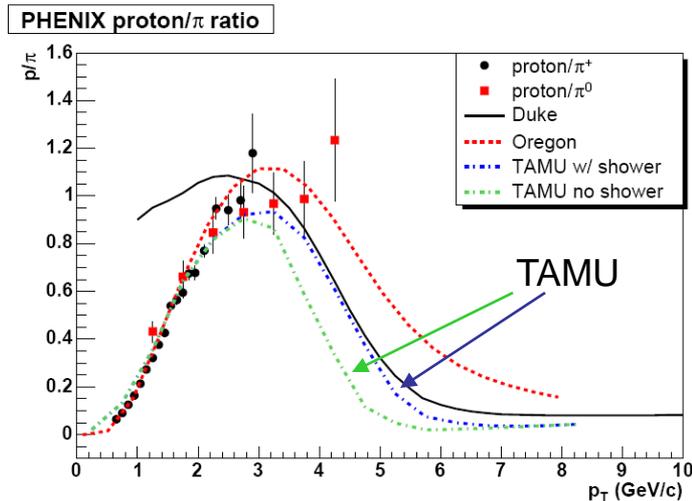


Fig. 53. The proton to pion ratio measured by PHENIX for Au+Au collisions at $\sqrt{s_{NN}} = 200$ GeV[52]. Several comparisons to recombination models as mentioned in the text are shown.

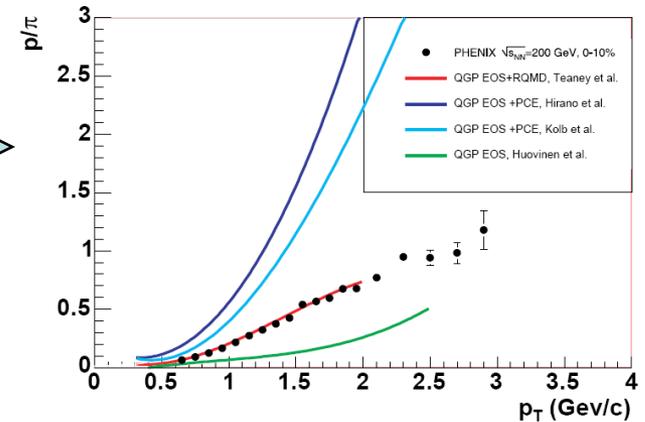


Fig. 52. p/π ratios for central (0–10%) Au+Au collisions at $\sqrt{s_{NN}} = 200$ GeV[52] compared to hydrodynamic models [106,107,117,118,119].



Recombinaison :

Prédit que le flot collectif des hadrons doit suivre le flot collectif de leur quarks constituants

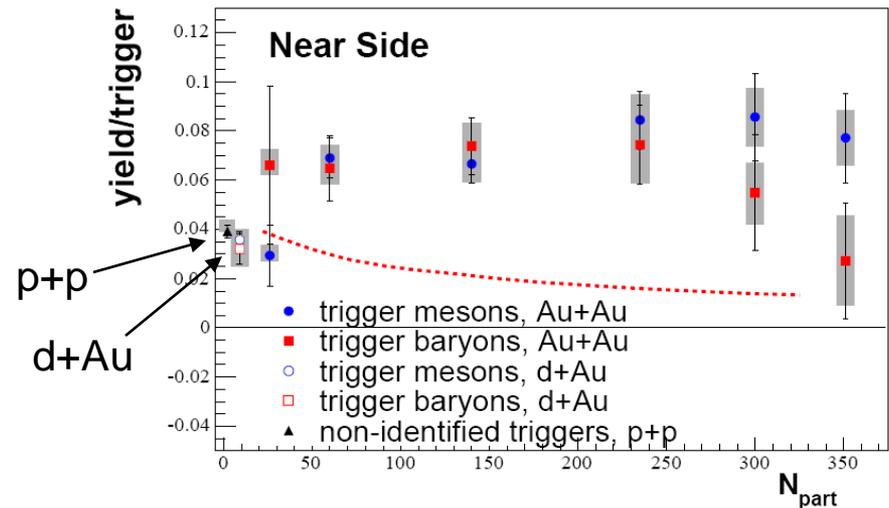
V. Production des hadrons de l'étude de l'hadronisation

4. Corrélations des jets

A crucial test of the origin for the enhanced (anti)proton to pion ratio is to see if baryons in this intermediate p_T regime exhibit correlations characteristic of the structure of jets from hard-scattered partons.

Mesure des jets :

- Compter le nombre de hadrons chargés (particules associées) dans un cône autour de la particule déclenchante
- particules déclenchantes : $2.5 < p_T < 4$
- particules associées : $1.7 < p_T < 2.5$



- Comportement similaire p+p et d+Au
- 2× plus de particules produites en AuAu → le processus de fragmentation est modifié par le milieu
- Dans les modèles de recombinaison, on s'attend à une baisse de « yield/trigger » (ligne pointillée)

V. Production des hadrons de l'étude de l'hadronisation

- Conclusions

The large (anti) baryon to pion excess relative to expectations from parton fragmentation functions at intermediate $p_T = 2 - 5 \text{ GeV}/c$ remains one of the most striking unpredicted experimental observations at RHIC. The data clearly indicate a new mechanism other than universal parton fragmentation as the dominant source of baryons and anti-baryons at intermediate p_T in heavy ion collisions. The boosting of soft physics, that dominates hadron production at low p_T , to higher transverse momentum has been explored with the context of hydrodynamic and recombination models. However, investigations into these intermediate p_T baryons reveals a near-angle correlation between particles, in a fashion characteristic of jet fragmentation. If instead these baryons have a partonic hard scattering followed by fragmentation source, this fragmentation process must be significantly modified. It is truly remarkable that these baryons have a large v_2 (typically 20%) indicative of strong collective motion and also a large “jet-like” near-side partner yield. At present, no theoretical framework provides a complete understanding of hadron formation in the intermediate p_T region.

Conclusions du White Paper

- **Densité d'énergie et particules chargées**
 - Densité d'énergie $\rightarrow 15 \text{ GeV/fm}^3$
 - Particules chargées \rightarrow saturation des gluons dans l'état initial ?
- **Thermalisation**
 - Production d'étrangeté en accord avec l'hypothèse d'un équilibre chimique.
 - Le flot elliptique observé indique un haut degré de collectivité.
 - Pas d'image consistante de la dynamique de la collision.
- **Binarité**
 - Effet Cronin en dAu \rightarrow CGC ?
 - Binarité des photons directs et du charme en AuAu \rightarrow compatible avec CGC ?
- **Suppression à grand pT**
 - Suppression des hadrons croissante avec la centralité \rightarrow milieu dense
 - Hypothèse d'un milieu dense confirmée par les corrélations angulaires
- **Production des hadrons**
 - Différence de comportement protons/pions
 - Étude du méson $\Phi \rightarrow$ différence de comportement pas liée à la différence de masse
 - Observation d'un flot partonique \rightarrow différence de comportement liée au nombre de quarks
 - Corrélations des jets incompatibles avec modèles de recombinaison

Les futures mesures de l'intérêt de continuer

- Suppression à grand p_T et physique des jets
 - Augmenter la statistique
 - Atteindre de plus grand p_T
- Production du J/Ψ
 - Jusqu'ici, shadowing mesuré en dAu, mais pas assez de statistique en AuAu
 - 1^{er} résultats attendus avec les données AuAu (2004) et CuCu (2005) → QM05.
 - Résultats à grande statistique avec les données AuAu (2008).
- Production du charme
 - Flot du charme
 - Perte d'énergie du charme dans un milieu dense
- Di-leptons de basse masse
 - Tester la restauration de la symétrie chirale (r,F,w/cf CERES au CERN)
 - Nouveau détecteur pour réduire le bruit de fond.
- Radiation thermique
 - Mesure des photons directs
 - Données 2004 → grande (suffisante ?) statistique